JACS
JOURNAL OF THE AMERICAN CHEMICAL SOCIETY
Article
pubs.acs.org/JACS

A Coupled Protein and Probe Engineering Approach for Selective Inhibition and Activity-Based Probe Labeling of the Caspases

Junpeng Xiao,[†] Petr Broz,[‡] Aaron W. Puri,[§] Edgar Deu,[†] Montse Morell,[†] Denise M. Monack,[‡] and Matthew Bogyo[†,*,‡]

Departments of [†]Pathology, [‡]Microbiology and Immunology, and [§]Chemical and Systems Biology, Stanford University School of Medicine, Stanford, California 94305, United States

Supporting Information

ABSTRACT: Caspases are cysteine proteases that play essential roles in apoptosis and inflammation. Unfortunately, their highly conserved active sites and overlapping substrate specificities make it difficult to use inhibitors or activity-based probes to study the function, activation, localization, and regulation of individual members of this family. Here we describe a strategy to engineer a caspase to contain a latent nucleophile that can be targeted by a probe containing a suitably placed electrophile, thereby allowing specific, irreversible inhibition and labeling of only the engineered protease. To accomplish this, we have identified a non-conserved residue on the small subunit of all caspases that is near the substrate-binding pocket and that can be mutated to a non-catalytic cysteine residue. We demonstrate that an active-site probe containing an irreversible binding acrylamide electrophile can specifically target this cysteine residue. Here we validate the approach using the apoptotic mediator, caspase-8, and the inflammasome effector, caspase-1. We show that the engineered enzymes are functionally identical to the wild-type enzymes and that the approach allows specific inhibition and direct imaging of the engineered targets in cells. Therefore, this method can be used to image localization and activation as well as the functional contributions of individual caspase proteases to the process of cell death or inflammation.

INTRODUCTION

Caspases are a family of cysteine proteases that play essential roles in both the regulation of apoptotic cell death and the inflammatory process known as pyroptosis. All caspases are synthesized as inactive zymogens that are converted into their active forms in response to cell death or inflammatory stimuli.[1,2] Upon induction of apoptosis, the initiator caspases (caspase-2, -8, -9, and -10) are assembled into multi-protein complexes such as PIDDosomes, DISCs, or apoptosomes. The active initiator caspases then cleave and activate downstream executioner caspases (caspase-3, -6, and -7), which process many substrates that are required to induce apoptotic cell death.[1,3,4] In response to infection or endogenous danger signals, caspase-1 is recruited to the inflammasome, where it is activated and promotes the processing of inflammatory cytokines and the induction of pyroptotic cell death.[2,5] Caspases can also be negatively regulated by degradation, post-translational modification, and binding of endogenous inhibitors.[6] These complex post-translational controls make it difficult to study the dynamic regulation of these proteases using classical cell biological or biochemical methods. Furthermore, the overall high degree of similarity within the active sites of caspases coupled with overlapping substrate preferences has made the development of selective inhibitors difficult.

Regardless of these challenges, several classes of activity-based probes (ABPs) have been developed to directly monitor caspase activation *in vitro* and *in vivo*. Commercially available FLICA (fluorescent labeled inhibitor of caspases) probes have been used in a number of cell biological applications.[7] However, these probes produce high levels of non-specific background labeling as a result of their reactive fluoromethyl ketone (FMK) electrophile.[8,9] Recently, our group has developed caspase ABPs containing a less reactive acyloxymethyl ketone (AOMK) electrophile. These probes can be used to label caspases-3, -6, -7, and -9[10−12] and most recently caspase-1.[9] Although these AOMK-containing probes are substantially more selective for caspases compared to FLICA probes, they still have some level of cross-reactivity with other cysteine proteases, including cathepsins and legumain. Moreover, all the current probes label multiple caspases simultaneously due to overlapping substrate preferences, and efforts to make them more selective for individual family members have proven difficult.[10] Therefore, although the current caspase ABPs are valuable tools for biochemical studies of multiple caspases, their lack of specificity within the family does not allow them to be used to inhibit or image a single caspase of interest.

In order to overcome this limitation in the use of small-molecule inhibitors and active-site probes of caspases, we have developed an approach that involves the co-engineering of a protease target and probe pair to produce a specific covalent interaction. The probe contains a reversible binding electrophile such as an aldehyde to drive initial association with the active-site cysteine but also contains a secondary electrophile that irreversibly forms a covalent bond when bound in close proximity to the engineered, non-catalytic cysteine (Figure 1). This approach takes advantage of the reactivity of cysteine as a latent nucleophile, as has been demonstrated for several

Received: April 9, 2013
Published: May 23, 2013

dx.doi.org/10.1021/ja403521u | J. Am. Chem. Soc. 2013, 135, 9130−9138

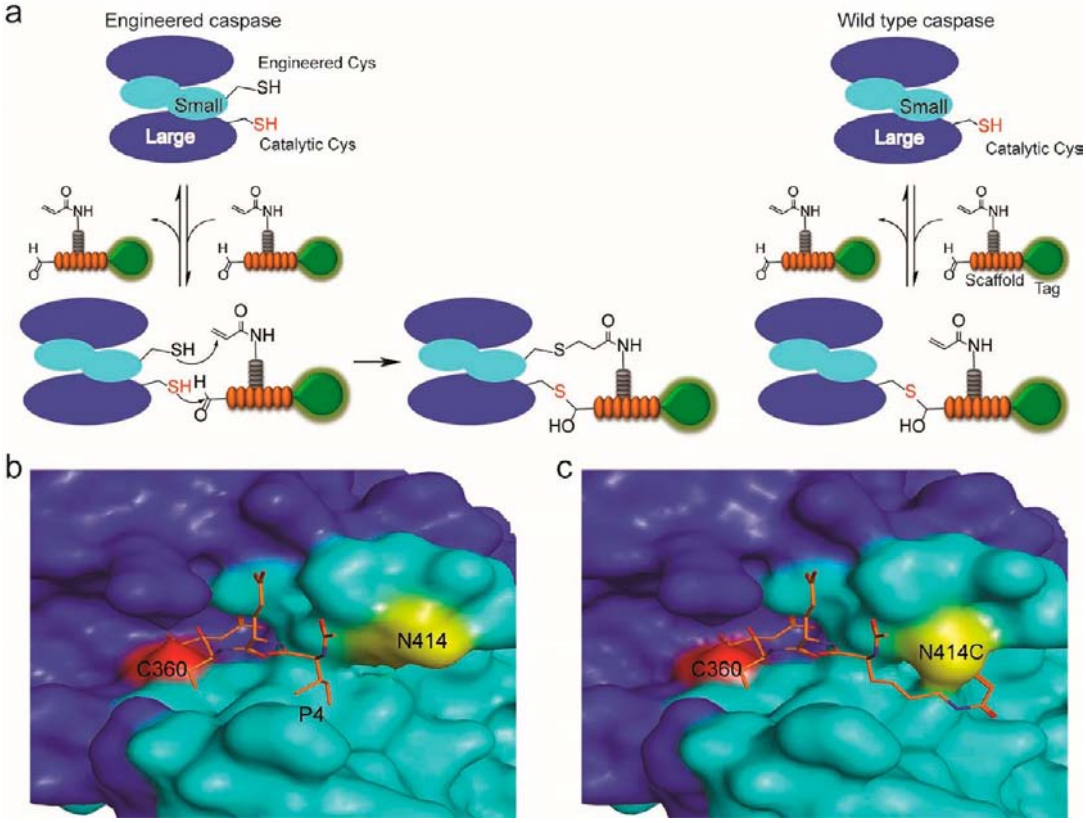

Figure 1. Development of activity-based probes that target a specific caspase. (a) Schematic representation of the caspase engineering and probe design method. The target caspase is engineered by introduction of a non-catalytic cysteine on the small subunit (cyan) such that it is near the substrate binding pocket. The designed probe contains an aldehyde electrophile at the C-terminus of the peptide scaffold (orange) for binding to the active-site cysteine on the large subunit (blue), an acrylamide electrophile on the peptide side chain (gray) for targeting the engineered cysteine, and a fluorescent tag (green) for detection. When the aldehyde reversibly binds to the catalytic cysteine, the acrylamide is placed in close proximity to the engineered cysteine, resulting in the irreversible formation of a stable probe/protease adduct. Binding between the probe and any wild-type caspase lacks the secondary covalent reaction and is therefore reversible. (b) Surface representation of the structure of the Ac-IETD-aldehyde bound to caspase-8 (PDB code: 1QTN). The large subunit is shown in blue, and the small subunit is shown in cyan. The Ac-IETD-aldehyde is shown as orange sticks. The catalytic cysteine is highlighted in red, and the mutation site is highlighted in yellow. (c) Surface representation of the modeled structure of the engineered caspase-8 N414C bound to a designed probe (orange).

applications including tag-based labeling of proteins,[13−15] selective kinase inhibition[16,17] and targeting of a serine protease containing a naturally occurring, non-catalytic cysteine.[18] Thus, we believed that this approach could be applied as a way to distinguish the functions of closely related caspases such as initiator caspase-8 vs caspase-10, executioner caspase-3 vs caspase-7, and inflammatory caspase-1 vs caspase-11, which are difficult to selectively label and inhibit by current ABPs and inhibitors. Here, we validate our approach using both an initiator caspase (caspase-8) and an inflammatory caspase (caspase-1). These data show the robustness of the approach and suggest that, in addition to these two protease targets, this strategy can likely be used to selectively target other caspases as well as other classes of proteolytic enzymes.

MATERIALS AND METHODS

Synthesis of Probes. The details of the synthesis of all probes can be found in the Supporting Information.

Recombinant Caspases, Enzyme Kinetics, and Substrate Specificity. The construct (pET15b-casp-8) for expression of caspase-8 (fragment 217−479) was provided by the Salvesen lab (Sanford Burnham Medical Research Institute). The constructs (pREST-casp-1 p20 and pREST-casp-1 p10) for expression of caspase-1 p20 subunit (fragment 120−297) and p10 subunit (fragment 317−404) were provided by the Wells lab (UCSF). Mutants were generated by overlap extension PCR.[19] The details are described in Supporting Information. Recombinant caspase-8 WT, N414C mutant, and C360S N414C double mutant were expressed and purified as described previously.[20] Recombinant caspase-1 WT and H342C mutant were expressed, refolded, and purified as described previously.[21] Active-site concentrations of purified proteins were determined by titration with irreversible inhibitors (AB20 for caspase-8 and Ac-YVAD-AOMK for caspase-1), and V_{max} and K_m values were determined using fluorogenic substrates (Ac-IETD-AFC for caspase-8 and Ac-WEHD-AMC for caspase-1) as described previously.[20] Sequence specificity was determined by screening positional scanning combinatorial AOMK inhibitor libraries as described previously.[10]

Molecular Modeling. All modeling was performed using the Molecular Operating Environment (MOE) software with the default energy minimization setting. The crystal structure of human caspase-8 bound to Ac-IETD-CHO inhibitor (PDB code: 1QTN) was used as the parent model. The N414C mutation and the p4 side chain on the inhibitor were manually modified, followed by energy minimization to obtain the modeled structure of engineered caspae-8 bound to the designed probe.

Inhibition of Caspase-8 with XJP027. Recombinant WT and N414C caspase-8 (10 nM) were incubated with increasing concentrations of XJP027 in caspase buffer [20 mM Pipes, 100 mM NaCl, 10 mM dithiothreitol (DTT), 1 mM EDTA, 0.1% Chaps, 10% sucrose, pH 7.2] at 37 °C in a 96-well plate. After a 15 min incubation, 50 μM Ac-IETD-AFC was added, and the initial rates (V_0) of substrate hydrolysis were determined by fluorescent detection using a plate

dx.doi.org/10.1021/ja403521u | J. Am. Chem. Soc. 2013, 135, 9130−9138

reader (λ_{abs} 495 nm, λ_{em} 515 nm) at 37 °C for 30 min. V_0 values were converted to percentages of residual activity relative to untreated controls. The IC_{50} values were determined by KaleidaGraph using sigmoidal fit. The final presented IC_{50} values represent the average of three independent assays.

Reversibility of XJP027 Inhibition. Recombinant WT and N414C caspase-8 (100 nM) were incubated with or without 1 μM XJP027 in caspase buffer at 37 °C for 30 min. After incubation, half of the samples were loaded onto a Ni-NTA column and washed with 50 mM sodium phosphate pH 7.5/5 mM DTT once and eluted with 50 mM sodium phosphate pH 7.5/250 mM imidazole/5 mM DTT. The concentrations of eluted proteins were determined by BCA protein assay. The percentages of residual activity of caspase-8 that were untreated, XJP027-treated, or XJP027 treated and then purified were determined as described above.

Labeling of Recombinant Caspases. Recombinant caspases (10 nM) were mixed with 1 mg/mL of cell lysates (NB7 cell lysate for caspase-8; *Casp1*$^{-/-}$ BMM cell lysate for caspase-1) in caspase buffer. The protein samples were pre-incubated with or without appropriate inhibitors (10 μM AB20 for caspase-8, 10 μM Ac-YVAD-AOMK for caspase-1, 15 mM NEM for all caspases) at 37 °C for 15 min. The appropriate probes (XJP027 for caspase-8; XJP062 for caspase-1) were added to the samples at the indicated concentrations and incubated at 37 °C for 1 h. After incubation, the samples were quenched with 4× SDS sample buffer and resolved by SDS-PAGE. The labeled proteins were visualized by in-gel fluorescence scanning using a flatbed laser scanner.

Time Course of XJP027 Labeling of Recombinant Caspase-8. Recombinant caspase-8 (10 nM) was added to NB7 cell lysate (1 mg/mL) in caspase buffer and incubated at 37 °C for 15 min. XJP027 (30 nM) was added to the samples. At the indicated time points, 30 μL aliquots were quenched with 10 μL of 4× SDS sample buffer and boiled at 100 °C for 5 min. The samples were resolved by SDS-PAGE and visualized by in-gel fluorescence scanning using a flatbed laser scanner.

NB7 Cell Culture and Transfections. NB7 cells were cultured in RPMI-1640 supplemented with 10% FBS, 2 mM L-glutamine, 100 U/mL penicillin, and 100 μg/mL streptomycin and maintained in 5% CO_2 incubator at 37 °C. The details of construction of pcDNA3 encoding procaspase-8 N414C are described in the Supporting Information. NB7 cells in RPMI-1640 supplemented with 10% FBS were seeded in six-well plates at 1.5×10^5 cells/well the day before transfection. Cells were transfected with 1 μg of plasmids using Nanojuice transfection reagent (EMD Bioscience) according to the manufacturer's instructions. The medium was changed to RPMI-1640 without supplement 4 h post-transfection.

LE37 Labeling of NB7 Cell Lysates. NB7 cells were harvested 9 h post-transfection and lysed with NP-40 lysis buffer (1% NP-40, 10 mM HEPES pH 7.4, 10 mM KCl, 5 mM $MgCl_2$, 2 mM EDTA, 2 mM DTT) on ice for 20 min. Cell lysates were clarified by centrifugation at 14K rpm for 20 min. Cell lysates were incubated with 0.5 μM LE37 at 37 °C for 30 min. The samples were resolved by SDS-PAGE and visualized by in-gel fluorescence scanning using a flatbed laser scanner.

XJP027 Labeling of Intact NB7 Cells. XJP027 (2 μM) was added into each well of transfected NB7 cells at 8 h post-transfection. The cells were incubated in 5% CO_2 incubator at 37 °C for 1 h. Cells were harvested and lysed with NP-40 lysis buffer. Cell lysates were resolved by SDS-PAGE and visualized by in-gel fluorescence scanning using a flatbed laser scanner.

Microscopy of XJP027 Labeling of NB7 Cells. NB7 cells were seeded on poly-Lys-coated glass coverslips in six-well plates and transfected as described above. Cells were labeled 5 h post-transfection with 5 μM XJP027 for 1 h. After labeling, cells were washed with medium three times (10 min each wash) at 37 °C and fixed with 4% paraformaldehyde in PBS for 30 min at room temperature. Cells were then washed with PBS three times (5 min each wash) and blocked with block buffer (0.3% Triton X-100, 5% rabbit serum in PBS) at room temperature for 1 h. Next the cells were incubated with an antibody specific for cleaved caspase-3 (1:1000 dilution, Cell Signaling Technology #9661) in antibody buffer (0.3% Triton X-100, 3% BSA in PBS) at 4 °C. After overnight incubation, cells were washed with PBS three times (5 min each wash) and incubated with Alexa-594 conjugated secondary antibody (1:1000 dilution, Invitrogen) in antibody buffer at room temperature for 1 h. Cells were then washed with PBS three times (5 min each wash) and mounted with mounting buffer containing DIPA. Images were obtained using a Zeiss Axiovert 200M microscope.

Generation of Immortalized BMMs. The immortalized wild-type (WT) BMMs and *Casp1*$^{-/-}$ BMMs were generated previously.[22] The details of construction of pMSCV2.2-IRES-GFP encoding murine procaspase-1 H340C mutant are described in Supporting Information. The immortalized pro-caspase-1 H340C BMMs were generated by transduction of immortalized *Casp1*$^{-/-}$ BMMs with vesicular stomatitis virus pseudotyped virus packaged in GP2 cells as described previously.[22]

BMM Culture and Infection. Immortalized BMMs were cultured in RPMI-1640 supplemented with 10% FBS, 2 mM L-glutamine, 100 U/mL penicillin, and 100 μg/mL streptomycin and maintained in 5% CO_2 incubator at 37 °C. Immortalized BMMs in RPMI-1640 supplemented with 10% FBS were seeded the day before infection in 6-well plates at 1.5×10^6 cells/well. *S. typhimurium* SL1344 was grown overnight in LB medium at 37 °C and then sub-cultured for 4 h prior to infection (10:1 MOI). The OD_{600} of sub-cultured *S. typhimurium* was measured, and the *S. typhimurium* was diluted to appropriate density in medium. The medium of overnight-cultured BMMs was removed, and *S. typhimurium* was added. The infections were synchronized by centrifugation of the *S. typhimurium* onto the cell monolayer at 500 *g* for 5 min.

Probe Labeling Infected BMMs. Probes (1 μM AWP28, 2.5 μM XJP062) were added to the infected immortalized BMMs. BMMs were labeled for the final hour of infection at 37 °C prior to sample preparation. After labeling, cells were washed with PBS once and lysed directly with 50 μL of 1× SDS sample buffer. The samples were resolved by SDS-PAGE and visualized by in-gel fluorescence scanning using a flatbed laser scanner.

Lactate Dehydrogenase (LDH) Release Assay. Immortalized BMMs were seeded in triplicate the day before infection in a 96-well plate at 3×10^4 cells/well. After infection (10:1 MOI), the supernatant was transferred to a new 96-well plate at indicated time points. The cells were lysed with 1× lysis buffer in medium for 1 h at 37 °C. The LDH activity of the supernatant and the lysate was measured using the CytoTox 96 Non-Radioactive Cytotoxicity Assay Kit (Promega). The percentage of LDH release was calculated as supernatant LDH activity/(supernatant LDH activity + lysate LDH activity).

Microscopy of XJP062 Labeling Infected BMMs. Immortalized BMMs were seeded on glass coverslips in 24-well plates at a density of 1.5×10^5 cells/well. Following *S. typhimurium* infection (10:1 MOI) and labeling with XJP062 (5 μM) for 1 h, the cells were washed with medium at 37 °C for 5 min. The cells were then washed with PBS once and fixed with 4% paraformaldehyde in PBS for 15 min at 37 °C. Cells were washed with PBS three times (5 min each wash) and blocked with block buffer (0.1% Triton X-100, 3% BSA in PBS) at room temperature for 30 min. Next the cells were incubated with an antibody specific for caspase-1 p10 subunit (1:100 dilution, Santa Cruz Biotechnology, sc-514) in block buffer at room temperature for 30 min. Cells were washed with PBS three times (5 min each wash) and incubated with Alexa-488-conjugated secondary antibody (1:500 dilution, Invitrogen) in block buffer at room temperature for 30 min. Cells were then washed with PBS four times (5 min each wash) and mounted with mounting buffer containing DAPI. Images were obtained using a Zeiss Axiovert 200M microscope.

RESULTS

Engineering Caspase-8. We initially chose to validate our engineering method using the initiator apoptotic caspase, caspase-8. This protease is activated by extrinsic signals that result in dimerization of the protease and subsequent processing from an inactive zymogen to the active protease.[23] This is an interesting initial target because it has both apoptotic

and additional non-apoptotic functions.[24] Our group has attempted to develop specific small-molecule inhibitors of this protease. However, all of the caspase-8 targeted compounds that we developed also inhibited other caspases, thus limiting their applications in cells and *in vivo*.[10]

Based on the crystal structure of recombinant human caspase-8 bound to the acetyl-Ile-Glu-Thr-Asp-aldehyde (Ac-IETD-CHO) inhibitor,[25] we chose Asn414 on the small subunit of caspase-8 as our top candidate for introduction of the cysteine. This residue is located on the small subunit that does not contain the catalytic cysteine but is an ideal location because it is near the active site and points toward the P4 position of the inhibitor, where an electrophile can be added (Figure 1b). In addition, Asn414 is not conserved among the caspases, suggesting that mutation of this residue is not likely to alter the function of the protease (Figure S1, Supporting Information). We therefore recombinantly expressed the WT caspase-8 and N414C mutant catalytic domains (fragment 217−479) containing an N-terminal His-tag. Ni-NTA purification of both the WT and the N414C yielded the mature, cleaved complex containing the large and small subunits, p18 and p10 (Figure S2, Supporting Information), indicating that, like WT caspase-8, the engineered caspase N414C mutant is active and able to auto-process.[26] We further assayed the activity of the WT and N414C enzymes using the Ac-IETD-AFC fluorogenic substrate. Importantly, the engineered cysteine variant retained WT activity, with both V_{max} (2535 RFU/min) and K_m (23.2 μM) values that were nearly identical to those of the WT enzyme (2829 RFU/min and 22.5 μM; Figure S3a, Supporting Information). Although both the WT and cysteine variant of caspase-8 had similar activity against a single fluorogenic substrate, we could not rule out the possibility that the mutation resulted in a change in the overall sequence selectivity of the enzyme. Therefore, we used a positional scanning library of peptide-based AOMK inhibitors that mimic protein substrates to assess any differences in binding preferences. These results confirmed that the N414C variant shared similar inhibitor specificity with the WT enzyme, suggesting that it would be likely to bind substrates with similar specificity as the WT enzyme (Figure S3b−d, Supporting Information).

Engineering a Selective Probe for the Engineered Caspase-8. For the design of a probe that targets the engineered caspase-8, we started with the classical peptide-based inhibitor, Ac-IETD-CHO, that contains a reversible binding aldehyde electrophile. We then used molecular modeling to determine where to attach a reactive acrylamide electrophile such that it would be in sufficient proximity to react with the engineered cysteine (Figure 1c). Thus, we designed the fluorescently labeled probe XJP027, which contains a KETD-aldehyde scaffold for reversible targeting of the catalytic Cys360, an acrylamide on the Lys side-chain in the P4 position for irreversible labeling of the engineered Cys414, and a carboxyfluorescein molecule at the N-terminus as a tag (Figure 2a). The probe was synthesized using solid-phase chemistry with H-Asp(OtBu)-aldehyde pre-loaded resin (Scheme S1, Supporting Information).

Validation of Specific Labeling and Irreversible Inhibition of the Engineered Caspase-8 *in Vitro*. In order to assess the ability of our probe to selectively and covalently modify the engineered caspase-8, we first performed labeling studies with 10 nM recombinant enzymes that were spiked into a cell lysate generated from the caspase-8-deficient cell line NB7.[27] Lysates were labeled with a range of concentrations of XJP027 (10 nM to 1 μM), and the samples were analyzed on SDS-PAGE followed by in-gel fluorescence scanning (Figure 2b). Remarkably, XJP027 showed no labeling of either WT caspase-8 or any other protein in the lysate at all concentrations tested. In contrast, we observed robust labeling of the N414C variant caspase-8 with saturation of labeling at concentrations as low as 30 nM. As expected, XJP027 labeled the p10 small subunit (~10 kDa) where we introduced the engineered cysteine. This labeling was completely inhibited by pre-incubation of the protein with the cysteine alkylating reagent *N*-ethylmaleimide (NEM; Figure 2b), confirming that the probe covalently labels the protease through the engineered cysteine. Additionally, we found that treatment with the previously reported caspase inhibitor AB20[10] or mutation of the active-site cysteine (C360S) blocked labeling of the engineered cysteine by XJP027 (Figure 2b and Figure S4a, Supporting Information), confirming that the probe requires

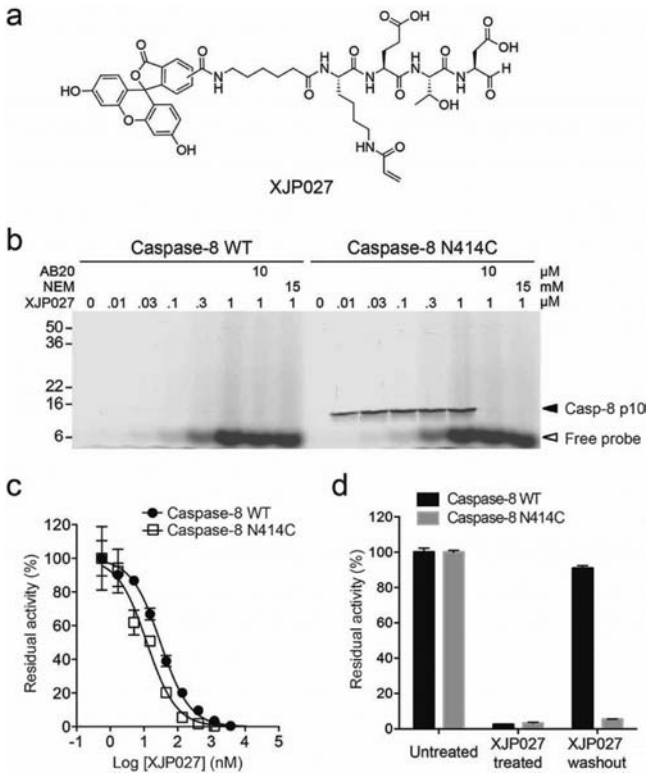

Figure 2. Specific labeling and irreversible inhibition of recombinant caspase-8 N414C. (a) Chemical structure of XJP027. (b) Recombinant WT or N414C caspase-8 (10 nM) in NB7 cell lysate (1 mg/mL) was pre-incubated with or without inhibitor (AB20 or NEM). Samples were labeled with XJP027 at the indicated concentrations and resolved by SDS-PAGE followed by in-gel fluorescence scanning using a flatbed laser scanner. The position of the caspase-8 p10 small subunit is indicated. (c) Recombinant WT and N414C caspase-8 (10 nM) were incubated with increasing concentrations of XJP027 for 15 min. The activity of treated caspase-8 was measured and plotted as the percent residual activity. Data are representative of three independent experiments. The IC_{50} values of XJP027 for WT and N414C caspase-8 are 32.6 ± 5.6 and 9.6 ± 3.5 nM, respectively. (d) Recombinant WT and N414C caspase-8 (10 nM) were treated with XJP027 (1 μM) and then re-purified with a Ni-NTA column to remove unbound or reversibly bound XJP027. Caspase activity was measured and plotted as the percent residual activity. Data are representative of three independent experiments.

dx.doi.org/10.1021/ja403521u | J. Am. Chem. Soc. 2013, 135, 9130−9138

initial direct interaction with the catalytic cysteine in order to induce the reaction with the engineered cysteine. As a final test of the probe in lysates, we measured the kinetics of the labeling reaction. We found that, when used at a concentration of 30 nM, XJP027 produced a detectable signal within 2 min, and this labeling was saturated in less than 30 min (Figure S4b, Supporting Information). XJP027 is also a highly sensitive probe, with a detection limit of 1 nM caspase-8 N414C (Figure S4c, Supporting Information).

Finally, we performed inhibition studies with the recombinant enzymes to determine if our probe was able to irreversibly inhibit the engineered caspase. Not surprisingly, XJP027 potently inhibited WT caspase-8 (IC_{50} = 32.6 nM). However, it was 3.4-fold more potent against caspase-8 N414C (IC_{50} = 9.6 nM; Figure 2c), and, importantly, the inhibition of this engineered caspase was retained even after re-purification by a Ni-NTA column (Figure 2d). In contrast, the activity of WT caspase-8 was almost completely recovered after removal of XJP027 (Figure 2d). Overall, these data demonstrate that the probe acts as a reversible inhibitor of the WT enzyme but is a permanent irreversible inhibitor of the cysteine-engineered caspase.

Validation of Function and Specific Labeling of the Engineered Caspase-8 in Cells. NB7 cells do not express caspase-8[27] and are therefore refractory to apoptosis induced by extrinsic stimuli. However, caspase-8 overexpression in these cells leads to self-aggregation and spontaneous induction of apoptosis.[27,28] Therefore, to examine whether our engineered caspase-8 was functional in cells, we transfected NB7 cells with full-length WT and N414C caspase-8 and monitored activation of cell death pathways using the broad-spectrum caspase ABP LE37.[12] When NB7 cells were transfected with an empty pcDNA3 vector, we observed only a small amount of active caspase-3 activity that was probably due to apoptosis induced by the transfection reagent. However, when WT or N414C caspase-8 was overexpressed, we observed robust activation of the downstream executioner caspases (Figure 3a). Importantly, the extent of apoptosis activation as measured by caspase-3, -6, and -7 labeling was similar upon expression of either the WT or cysteine-engineered caspase-8, suggesting that the two are functionally equivalent.

We next wanted to determine if our probe was capable of specific labeling of the engineered protease in intact cells. Therefore, we added the probe to live NB7 cells that had been transfected with either WT or N414C caspase-8 and observed specific labeling of the p10 subunit only in cells that expressed the engineered caspase-8 (Figure 3b). These results confirmed that XJP027 was able to enter cells and produce highly specific labeling of its target. Importantly, XJP027 showed no background labeling in cells transfected with either pcDNA3 or WT caspase-8, again confirming the selectivity of the labeling reaction. As a final test of selectivity, we treated cells expressing either WT or N414C caspase-8 with the probe and then monitored inhibition by subsequent labeling of residual caspase activity with LE37 (Figure 3c). These results clearly demonstrated that the probe blocked the activity of only the engineered form of caspase-8, leaving all other caspase activities intact, thus confirming that it will be possible to use this method to selectively disrupt the activity of the engineered protease in intact cells.

One of the most powerful applications for ABPs is to directly visualize protease activity using optical imaging techniques. Therefore, we next performed labeling experiments in which

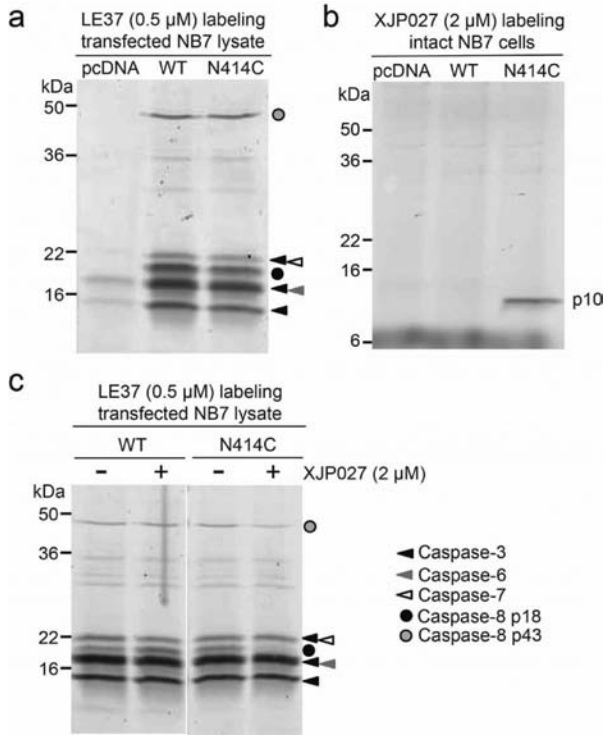

Figure 3. Specific labeling and inhibition of engineered caspase-8 in NB7 cells. (a) NB7 cells were transfected with the indicated vectors for 9 h. Cell lysates were labeled with the broad-spectrum caspase probe LE37 and analyzed by SDS-PAGE followed by in-gel fluorescence scanning. The location of the various caspases is indicated with symbols defined in the inset key. (b) NB7 cells were transfected, and intact cells were labeled with XJP027 1 h before harvesting. Harvested cells were lysed and analyzed by SDS-PAGE followed by in-gel fluorescence scanning. The location of the caspase-8 p10 small subunit is indicated. (c) Cell lysates from (b) were labeled with LE37 for 30 min and analyzed by SDS-PAGE followed by in-gel fluorescence scanning.

cells expressing either the WT or cysteine-engineered caspase-8 were incubated with the fluorescent probe and then visualized by microscopy. We also used an antibody for cleaved caspase-3 as a marker for cells that had undergone apoptosis as a result of expression of caspase-8 (Figure 4). Although the majority of NB7 cells transfected with WT caspase-8 were positive for cleaved caspase-3, they were not labeled by XJP027 (Figure 4). In contrast, NB7 cells transfected with caspase-8 N414C showed strong XJP027 labeling that co-localized with cleaved caspase-3 staining (Figure 4). These cell imaging results are consistent with the gel labeling results (Figure 3) and confirm that the engineered caspase-8 N414C is functional and can be specifically imaged by the designed ABP XJP027.

Development of a Specific Probe for Caspase-1. Having demonstrated the successful application of our approach for caspase-8, we next wanted to test the robustness of the method by targeting a different caspase using the same general approach. Recently, our group developed an optimized ABP for caspase-1 and showed the value of this reagent for biochemical studies of caspase-1 activation during pyroptosis.[9] However, this probe also targets caspase-3, caspase-7, and legumain. Based on sequence and structural alignments (Figures S1 and S5, Supporting Information), we found that His342 of caspase-1 (in the same position as Asn414 in caspase-8) was likely to be ideal for introduction of a cysteine

dx.doi.org/10.1021/ja403521u | J. Am. Chem. Soc. 2013, 135, 9130−9138

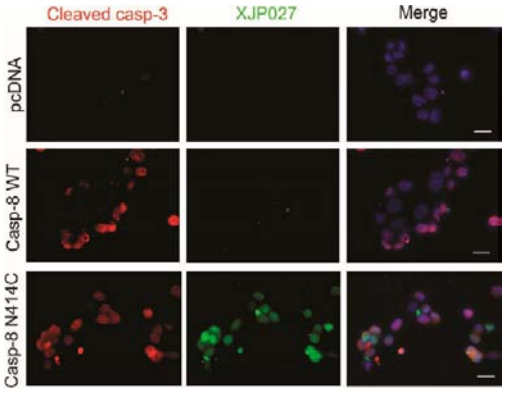

Figure 4. Fluorescence imaging of engineered caspase-8 in NB7 cells. NB7 cells were transfected with the indicated caspase-8 vectors for 6 h, followed by labeling with XJP027 (5 μM) for the final hour of transfection. Cells were washed, fixed, and stained with an antibody specific for cleaved caspase-3 (Alexa 594-conjugated secondary antibody) and with DAPI for nuclear staining. Cells were imaged for nuclei (blue), cleaved caspase-3 (red), and XJP027 (green). Scale bars are 25 μm.

mutation. We therefore produced recombinant human caspase-1 containing the H342C mutation and found that the enzyme had V_{max} values almost identical to those of the WT enzyme (4237 RFU/min for WT and 4219 RFU/min for H342C). However, we observed an increased K_m value (19.3 μM for WT and 94.0 μM for H342C; Figure S6a, Supporting Information), suggesting that the engineered caspase-1 retained the same catalytic rate but had reduced binding affinity for the Ac-WEHD-AMC substrate. However, like caspase-8, we found that the engineered caspase-1 had sequence specificity similar to that of the WT enzyme as measured using the positional scanning inhibitor library, suggesting that it likely retains its normal function toward substrates (Figure S6b–d, Supporting Information).

We next synthesized the probe XJP062 to pair with the engineered caspase-1 (Figure 5a and Scheme S2, Supporting Information). Like XJP027, XJP062 contains a peptide aldehyde scaffold, an acrylamide on the lysine side-chain at the P4 position, and a fluorescent tag (in this case Cy5). However, it contains the peptide VAD sequence that is more optimal for caspase-1. The specificity of XJP062 was tested with recombinant caspase-1, and again we observed specific labeling of the p10 subunit of engineered caspase-1, with saturation of labeling at 100 nM (Figure 5b). The labeling was also completely inhibited by pre-incubation with the caspase-1 inhibitor Ac-YVAD-AOMK[29] or the general cysteine alkylating agent NEM (Figure 5b). These data confirm that XJP062 is a specific activity-based probe that covalently labels H342C caspase-1 through the engineered cysteine.

Specific Labeling and Imaging of Engineered Caspase-1 in Murine BMMs. Our previous studies using AWP28 showed that both primary and immortalized murine bone marrow macrophages (BMMs) undergo rapid pyroptotic cell death when infected with *Salmonella enterica serovar typhimurium* (*S. typhimurium*). However, *Casp1*$^{-/-}$ BMMs induce an apoptotic cell death that could be restored to a pyroptotic cell death by re-introduction of a catalytically functional caspase-1.[9] Therefore, we could confirm that our engineered caspase-1 is functionally identical to the WT enzyme by re-introducing it into the *Casp1*$^{-/-}$ BMMs and then monitoring cell death upon *S. typhimurium* infection. We created immortalized *Casp1*$^{-/-}$ (i*Casp1*$^{-/-}$) BMMs that stably express the cysteine-engineered murine procaspase-1 (iH340C). Importantly, the expression level of the engineered caspase-1 in iH340C BMMs was similar to the endogenous levels of caspase-1 in immortalized wild-type (iWT) BMMs (Figure S7, Supporting Information). As shown previously,

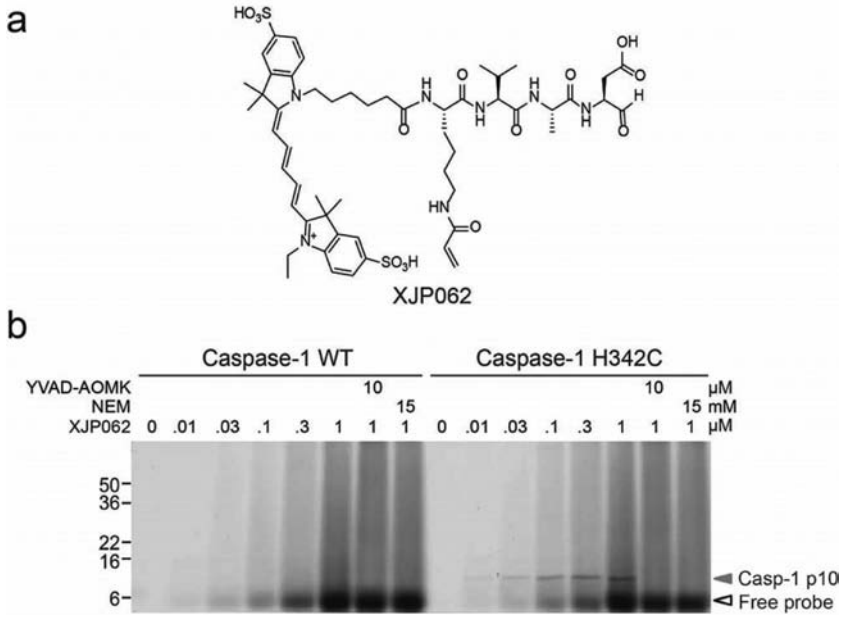

Figure 5. Specific labeling of recombinant engineered caspase-1. (a) Structure of XJP062. (b) Recombinant WT or H342C human caspase-1 (10 nM) that was added to *Casp1*$^{-/-}$ BMM cell lysate (1 mg/mL) was pre-incubated with or without inhibitor (Ac-YVAD-AOMK or NEM) for 15 min. Samples were labeled with XJP062 at the indicated concentrations for 1 h. The labeled samples were analyzed by SDS-PAGE, followed by in-gel fluorescence scanning. The location of the caspase-1 p10 small subunit is indicated.

dx.doi.org/10.1021/ja403521u | J. Am. Chem. Soc. 2013, 135, 9130–9138

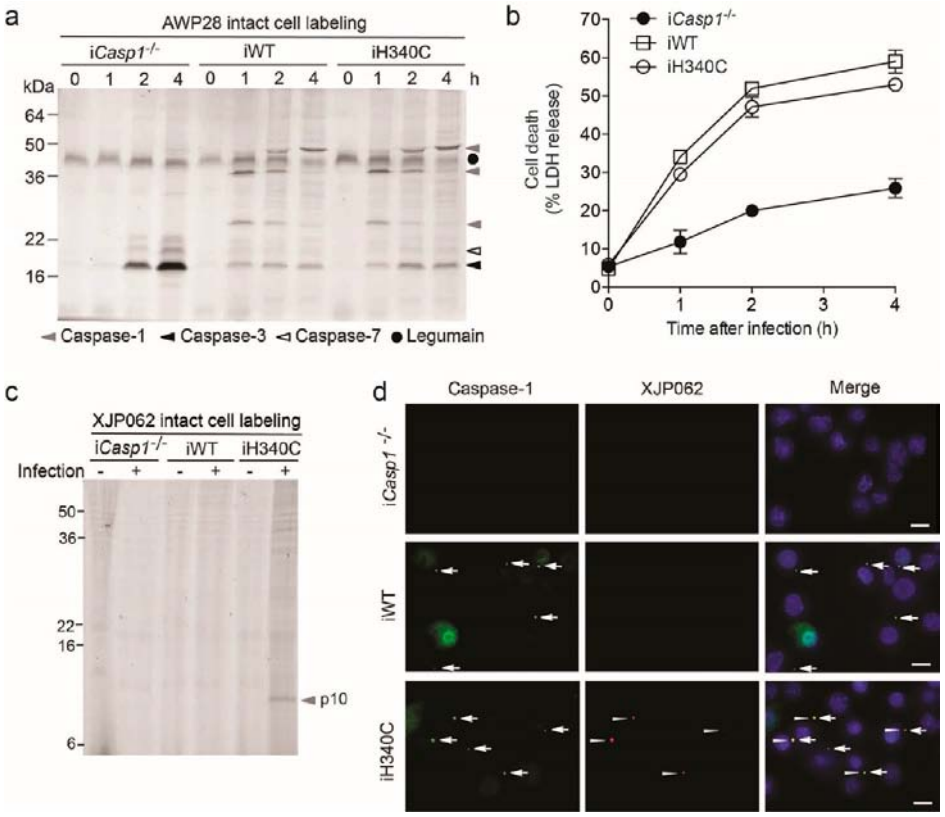

Figure 6. Engineered caspase-1 can induce pyroptosis and can be specifically labeled and imaged in intact cells. (a) Immortalized *Casp-1*$^{-/-}$ BMMs (i*Casp-1*$^{-/-}$), immortalized wild-type (iWT) BMMs, and *Casp-1*$^{-/-}$ BMMs expressing the murine caspase-1 H340C mutant (iH340C) were infected with *S. typhimurium* (10:1) and labeled with the caspase-1 probe AWP28 (1 μM) for the final hour of infection. At indicated time points, cells were lysed with 1× SDS sample buffer and analyzed by SDS-PAGE by in-gel fluorescence scanning. The locations of various intermediate forms of the large subunit of caspase-1 (containing the active-site cysteine but not the engineered cysteine) as well as other caspases and the off-target legumain are indicated with symbols that are defined in the key at the bottom of the gel. (b) Quantification of LDH release by cells in (a) upon *S. typhimurium* infection. (c) Immortalized BMMs were uninfected or infected with *S. typhimurium* (10:1) for 1 h and labeled with XJP062 (2.5 μM) for the final hour of infection. Cells were lysed with 1× SDS sample buffer and analyzed by SDS-PAGE followed by in-gel fluorescence scanning. The location of the labeled caspase-1 small p10 subunit containing the engineered cysteine is indicated. (d) *S. typhimurium* infected BMMs (10:1 MOI for 1 h) were labeled by XJP062 (5 μM) for 1 h. Cells were washed, fixed, and stained with a caspase-1 antibody/Alexa 488-conjugated secondary antibody and DAPI nuclear stain. Cells were imaged for nuclei (blue), caspase-1 (green), and XJP062 (red). Caspase-1 positive inflammasome foci are indicated with arrows. XJP062-labeled inflammasome foci are indicated with arrowheads. Scale bars are 10 μm.

upon *S. typhimurium* infection of *Casp1*$^{-/-}$ BMMs, we observed robust activation of caspase-3 and -7 and cell death by apoptosis (Figure 6a,b). However, upon expression of either WT or the H340C mutant caspase-1, we observed a shift back to pyroptotic death as detected by labeling of active caspase-1 by AWP28 (Figure 6a) and the rapid release of LDH (Figure 6b). These results confirm that the engineered caspase-1 is active and is capable of inducing pyroptosis in macrophages upon *S. typhimurium* infection. We also confirmed that XJP062 was able to specifically label the engineered caspase-1 in *S. typhimurium* infected macrophages. Again, probe addition to intact cells resulted in labeling of the p10 subunit with only several weak, non-specific background signals observed at higher molecular weight (Figure 6c).

We and others have previously shown that, during *S. typhimurium* infection, active caspase-1 is recruited into a single defined focus within the cell along with other components of the inflammasome, such as the apoptosis-associated speck-like protein containing a CARD (ASC). These foci can be visualized by ABP labeling and by fluorescent microscopic staining using caspase-1-specific antibodies.[22,30] Therefore, we could determine the selectivity of our probe for the engineered caspase by performing fluorescence microscopy studies in infected cells expressing either the WT or engineered caspase-1. As expected, i*Casp1*$^{-/-}$ BMMs showed no signal for either the XJP062 probe or the caspase-1 antibody (Figure 6d). However, we could observe specific staining of inflammasome foci by our probe in infected iH340C BMMs but not in iWT BMMs, even though the formation of the foci in both cell lines could be detected by staining with the anti-caspase-1 antibody (Figure 6d). Therefore, we could conclude that the engineered caspase-1 is functionally equivalent to WT caspase-1 and, furthermore, that our designed probe is able to selectively label the active pool of this engineered protease with absolute specificity over other caspases.

■ DISCUSSION

Caspase activity is post-translationally regulated. Therefore, small-molecule ABPs are useful tools to directly monitor the dynamic regulation of these proteases.[9−12] Unfortunately, all of the previously reported caspase probes lack specificity, thus preventing their application for imaging the activation and regulation of a specific caspase target. Using a coupled protein engineering and probe design approach, we were able to

dx.doi.org/10.1021/ja403521u | J. Am. Chem. Soc. 2013, 135, 9130−9138

develop activity-based probes that label and inhibit distinct engineered caspases. This approach makes use of a non-conserved residue at the S4 substrate binding pocket of the target caspase that can be mutated to a non-catalytic cysteine without altering the folding, activation, or substrate specificity of the caspase. This latent nucleophile can then be used to direct specificity toward a probe that contains a reactive electrophile. By creating a general approach that allows engineering of a probe/enzyme pair, it is possible to control the activity of a specific target protease and, at the same time, use the probe to image activity in a highly selective manner. In this study we demonstrate the utility of this approach using two distinct caspase family members, but we believe that this method can be broadened to other classes of proteases.

One of the most challenging aspects of the design method is finding a site on the target protease to introduce the cysteine mutation. The biggest concern is that making changes to the protease will result in changes in protein folding, substrate binding, or catalytic activity that could change the function of the enzyme. In this study, we have performed the engineering method on two distinct caspase family members. We have chosen a site on the small subunit that is non-conserved and therefore less likely to be important for the overall integrity of the enzyme. We found that, in both cases, we were able to generate mutant enzymes that have virtually identical activity against substrates *in vitro*. In addition, both mutant enzymes are functional in cells, suggesting that our chosen mutations have not altered the synthesis, stability, or folding of the enzyme. Most importantly, we show that the engineered caspase-1 is functionally equivalent to the WT enzyme when expressed in cells that have the caspase-1 gene deleted. Specifically, we find that WT and cysteine mutant caspase-1 are able to activate pyroptotic cell death to a similar extent and with similar overall kinetics (Figure 6b). This result confirms that it will be possible to introduce the mutant protease in place of the native enzyme without compromising the biological integrity of the system.

When designing the probes used in this study, we had to choose an electrophile that would react with the newly introduced cysteine without having overall broad reactivity toward any exposed free cysteine in the cell. We chose the acrylamide electrophile because it has been shown to have sufficient reactivity to perform rapid labeling of cysteine residues through a proximity-induced Michael addition reaction but is not reactive enough to label other intracellular nucleophiles.[14,31,32] The main drawback of this electrophile is that there is no direct leaving group, thus making it difficult to apply it to generate probes that are fluorescently quenched but that produce a fluorescent signal after reaction with the engineered cysteine. We believe that a next-generation quenched probe will be required in order to perform real-time or single-molecule fluorescence studies using this approach. We are currently working on several classes of new electrophiles for generation of quenched probes with improved properties for imaging.

Both *in vitro* labeling and cell labeling experiments have proven that the designed probes XJP027 and XJP062 are specific for engineered caspase-8 and caspase-1, respectively. Although the probes also bound to WT caspases via a reversible bond between the aldehyde and the catalytic cysteine, this inhibition is reversed by washing the cells to remove the probe. Therefore, we were able to permanently inhibit the engineered target with absolute selectivity. We also show that the labeling of the engineered target is rapidly saturated, thus allowing studies of caspase function within a timeline that is suitable for the events of interest during apoptosis.

CONCLUSION

In conclusion, we developed an approach to inhibit and label specific caspases using a paired protein engineering and probe design approach. The same approach was taken to develop specific probes for matrix metalloproteinases (MMPs; see companion paper[38]), suggesting that this is a general method that can be applied to a variety of protease families. Although our approach requires genomic engineering of the target protein, techniques for site-specific genome editing using zinc-finger nucleases (ZFNs), transcription activator-like effector nucleases (TALENs), and clustered regularly interspaced short palindromic repeat (CRISPR)/Cas system have recently been developed.[33−37] Using these methods, the endogenous proteases can be engineered in cells or even in animals. Therefore, we believe our approach has the potential to be broadly used for studying the activation and regulation of a variety of protease targets in complex and biologically relevant systems.

ASSOCIATED CONTENT

Supporting Information

Figures S1−S7, Schemes S1 and S2, and supplementary materials and methods. This material is available free of charge via the Internet at http://pubs.acs.org.

AUTHOR INFORMATION

Corresponding Author

mbogyo@stanford.edu

Notes

The authors declare no competing financial interest.

ACKNOWLEDGMENTS

We thank the members of Bogyo lab for useful discussions. LE37 was provided by Laura Edgington. NB7 cells and the plasmids for recombinant caspase-8 WT expression and pcDNA3 encoding procaspase-8 were provided by the Salvesen lab (Sanford Burnham Medical Research Institute). The plasmids for recombinant caspase-1 WT expression were provided by the Wells lab (UCSF). This work was supported by National Institutes of Health grants R01 EB005011 and R21 EB012311-01 (to M.B.). M.M. was supported by AGAUR through the Beatriu de Pinos program.

REFERENCES

(1) Denault, J. B.; Salvesen, G. S. *Chem. Rev.* **2002**, *102*, 4489.
(2) Bergsbaken, T.; Fink, S. L.; Cookson, B. T. *Nat. Rev. Microbiol.* **2009**, *7*, 99.
(3) Budihardjo, I.; Oliver, H.; Lutter, M.; Luo, X.; Wang, X. *Annu. Rev. Cell Dev. Biol.* **1999**, *15*, 269.
(4) MacKenzie, S. H.; Clark, A. C. *Adv. Exp. Med. Biol.* **2012**, *747*, 55.
(5) Miao, E. A.; Rajan, J. V.; Aderem, A. *Immunol. Rev.* **2011**, *243*, 206.
(6) Pop, C.; Salvesen, G. S. *J. Biol. Chem.* **2009**, *284*, 21777.
(7) Bedner, E.; Smolewski, P.; Amstad, P.; Darzynkiewicz, Z. *Exp. Cell Res.* **2000**, *259*, 308.
(8) Pozarowski, P.; Huang, X.; Halicka, D. H.; Lee, B.; Johnson, G.; Darzynkiewicz, Z. *Cytometry A* **2003**, *55*, 50.
(9) Puri, A. W.; Broz, P.; Shen, A.; Monack, D. M.; Bogyo, M. *Nat. Chem. Biol.* **2012**, *8*, 745.
(10) Berger, A. B.; Witte, M. D.; Denault, J. B.; Sadaghiani, A. M.; Sexton, K. M.; Salvesen, G. S.; Bogyo, M. *Mol. Cell* **2006**, *23*, 509.

(11) Edgington, L. E.; Berger, A. B.; Blum, G.; Albrow, V. E.; Paulick, M. G.; Lineberry, N.; Bogyo, M. *Nat. Med.* **2009**, *15*, 967.
(12) Edgington, L. E.; van Raam, B. J.; Verdoes, M.; Wierschem, C.; Salvesen, G. S.; Bogyo, M. *Chem. Biol.* **2012**, *19*, 340.
(13) Krusemark, C. J.; Belshaw, P. J. *Org. Biomol. Chem.* **2007**, *5*, 2201.
(14) Gallagher, S. S.; Sable, J. E.; Sheetz, M. P.; Cornish, V. W. *ACS Chem. Biol.* **2009**, *4*, 547.
(15) Chen, Z.; Jing, C.; Gallagher, S. S.; Sheetz, M. P.; Cornish, V. W. *J. Am. Chem. Soc.* **2012**, *134*, 13692.
(16) Blair, J. A.; Rauh, D.; Kung, C.; Yun, C. H.; Fan, Q. W.; Rode, H.; Zhang, C.; Eck, M. J.; Weiss, W. A.; Shokat, K. M. *Nat. Chem. Biol.* **2007**, *3*, 229.
(17) Garske, A. L.; Peters, U.; Cortesi, A. T.; Perez, J. L.; Shokat, K. M. *Proc. Natl. Acad. Sci. USA.* **2011**, *108*, 15046.
(18) Hagel, M.; Niu, D., St; Martin, T.; Sheets, M. P.; Qiao, L.; Bernard, H.; Karp, R. M.; Zhu, Z.; Labenski, M. T.; Chaturvedi, P.; Nacht, M.; Westlin, W. F.; Petter, R. C.; Singh, J. *Nat. Chem. Biol.* **2011**, *7*, 22.
(19) Nelson, M. D.; Fitch, D. H. *Methods Mol. Biol.* **2011**, *772*, 459.
(20) Stennicke, H. R.; Salvesen, G. S. *Methods* **1999**, *17*, 313.
(21) Datta, D.; Scheer, J. M.; Romanowski, M. J.; Wells, J. A. *J. Mol. Biol.* **2008**, *381*, 1157.
(22) Broz, P.; von Moltke, J.; Jones, J. W.; Vance, R. E.; Monack, D. M. *Cell Host Microbe* **2010**, *8*, 471.
(23) Zhao, Y.; Sui, X.; Ren, H. *J. Cell Physiol.* **2010**, *225*, 316.
(24) Maelfait, J.; Beyaert, R. *Biochem. Pharmacol.* **2008**, *76*, 1365.
(25) Watt, W.; Koeplinger, K. A.; Mildner, A. M.; Heinrikson, R. L.; Tomasselli, A. G.; Watenpaugh, K. D. *Structure* **1999**, *7*, 1135.
(26) Smith, G. K.; Barrett, D. G.; Blackburn, K.; Cory, M.; Dallas, W. S.; Davis, R.; Hassler, D.; McConnell, R.; Moyer, M.; Weaver, K. *Arch. Biochem. Biophys.* **2002**, *399*, 195.
(27) Teitz, T.; Wei, T.; Valentine, M. B.; Vanin, E. F.; Grenet, J.; Valentine, V. A.; Behm, F. G.; Look, A. T.; Lahti, J. M.; Kidd, V. J. *Nat. Med.* **2000**, *6*, 529.
(28) Torres, V. A.; Mielgo, A.; Barila, D.; Anderson, D. H.; Stupack, D. *J. Biol. Chem.* **2008**, *283*, 36280.
(29) Thornberry, N. A.; Peterson, E. P.; Zhao, J. J.; Howard, A. D.; Griffin, P. R.; Chapman, K. T. *Biochemistry* **1994**, *33*, 3934.
(30) Broz, P.; Newton, K.; Lamkanfi, M.; Mariathasan, S.; Dixit, V. M.; Monack, D. M. *J. Exp. Med.* **2010**, *207*, 1745.
(31) Levitsky, K.; Ciolli, C. J.; Belshaw, P. J. *Org. Lett.* **2003**, *5*, 693.
(32) Weerapana, E.; Simon, G. M.; Cravatt, B. F. *Nat. Chem. Biol.* **2008**, *4*, 405.
(33) Miller, J. C.; Tan, S.; Qiao, G.; Barlow, K. A.; Wang, J.; Xia, D. F.; Meng, X.; Paschon, D. E.; Leung, E.; Hinkley, S. J.; Dulay, G. P.; Hua, K. L.; Ankoudinova, I.; Cost, G. J.; Urnov, F. D.; Zhang, H. S.; Holmes, M. C.; Zhang, L.; Gregory, P. D.; Rebar, E. J. *Nat. Biotechnol.* **2011**, *29*, 143.
(34) Bedell, V. M.; Wang, Y.; Campbell, J. M.; Poshusta, T. L.; Starker, C. G.; Krug, Ii, R. G.; Tan, W.; Penheiter, S. G.; Ma, A. C.; Leung, A. Y.; Fahrenkrug, S. C.; Carlson, D. F.; Voytas, D. F.; Clark, K. J.; Essner, J. J.; Ekker, S. C. *Nature* **2012**, *491*, 114.
(35) Perez-Pinera, P.; Ousterout, D. G.; Gersbach, C. A. *Curr. Opin. Chem. Biol.* **2012**, *16*, 268.
(36) Sood, R.; Carrington, B.; Bishop, K.; Jones, M.; Rissone, A.; Candotti, F.; Chandrasekharappa, S. C.; Liu, P. *PLoS One* **2013**, *8*, e57239.
(37) Wang, H.; Yang, H.; Shivalila, C. S.; Dawlaty, M. M.; Cheng, A. W.; Zhang, F.; Jaenisch, R. *Cell* **2013**, *153*, 910.
(38) Morell, M.; Nguyen Duc, T.; Willis, A. L.; Syed, S.; Lee, J.; Deu, E.; Deng, Y.; Xiao, J.; Turk, B. E.; Jessen, J. R.; Weiss, S. J.; Bogyo, M. *J. Am. Chem. Soc.* **2013**, DOI: 10.1021/ja403523p.